

# SPATIAL 3D IMAGING BY SYNTHETIC AND DIGITIZED HOLOGRAPHY

*Yasuaki Arima<sup>1</sup>, Kyoji Matsushima<sup>1</sup>, and Sumio Nakahara<sup>2</sup>*

<sup>1</sup>Department of Electrical and Electronic Engineering, Kansai University

<sup>2</sup>Department of Mechanical Engineering, Kansai University

3-3-35 Yamate-cho, Suita, Osaka 564-8680, Japan. E-mail: matsu@kansai-u.ac.jp

## ABSTRACT

A novel method named digitized holography is proposed for 3D display systems. This is the technique replacing the whole process of classical holography with digital processing of optical wave-fields. The digitized holography allows us to edit holograms and reconstruct spatial 3D images including real-existent objects and CG-modeled virtual objects.

**Index Terms**—Holography, Digital recording, Optical imaging

## 1. INTRODUCTION

In classical holography, the object wave of a real-existent object is recorded on light-sensitive films by the interference with reference waves. This object wave is reconstructed by diffraction by the fringe pattern. However, recent development of polygon-based algorithms [1] makes it possible to synthesize the object wave of completely virtual 3D scenes provided by the CG model. The synthetic full-parallax holograms are created in extremely high-definition by using laser lithography system [2]. These holograms reconstruct true-fine spatial 3D images that are quite different from that by conventional 3D systems providing only binocular disparity.

In addition, recent evolution of image sensors and the technique for capturing large-scaled wave-fields [3] also makes it possible to digitize the whole process of the classical holography. We call this technique digitized holography. In contrast of the classical holography, the digitized holography allows us to freely edit the 3D scene and mix the real-existent objects with CG modeled virtual objects. The created hologram is an embodiment of digital data that can be archived and transmitted by digital media.

In this paper, we propose the full-synthetic and digitized holography, and demonstrate extremely high-definition holograms produced by the proposed techniques. The spatial 3D images reconstructed by these high-definition holograms give reviewers a strong sensation of depth that never has been caused by conventional 3D systems.

## 2. SYNTHETIC OBJECT FIELD BY POLYGON-BASED ALGORITHM

Full-synthetic holograms are usually called Computer-Generated Hologram (CGH). For a long time, the point-based method has been used for numerical synthesis of object fields in creating CGHs. In this method, the object surfaces are regarded as being covered up with much many point sources of light. The point-based method is simple to calculate but much time-consuming, especially in creation of full-parallax high-definition CGHs. To get over the problem, we recently presented the polygon-based method that remarkably reduces computation time [1,2].

### 2.1. Theoretical model of a polygonal surface source

In the polygon-based method, object surfaces are formed of polygonal planes (polygons) as shown in Fig.1 (a), and each polygon emits the wave-field. The light scattered by polygonal surfaces is similar to the field diffracted by an aperture that is irradiated with a plane wave, as shown in Fig. 2. The aperture has the same shape and slant as the polygon. However, a simple polygonal aperture may not behave as if it is a surface source of light, because the aperture size is too large to sufficiently diffract incident light. Therefore, the polygonal surface source is imitated by a virtual (numerical) diffuser that is mounted in the aperture whose shape and slant correspond with the polygon.

### 2.2. Surface functions

To compute the wave-field diffracted by the polygon-shaped diffuser, a local coordinates  $(x_n, y_n, z_n)$  is defined for each individual polygon, and a complex function is provided in the  $(x_n, y_n, 0)$  plane. This is called a surface function. An example of the surface function is shown in Fig. 1 (b).

The surface function  $h_n(x_n, y_n)$  for a polygon is generally given in the form:

$$h_n(x_n, y_n) = a_n(x_n, y_n) \exp[i\phi_n(x_n, y_n)],$$

where  $a_n(x_n, y_n)$  and  $\phi_n(x_n, y_n)$  are the real-valued amplitude and phase distribution in the local coordinates. The phase pattern  $\phi_n(x_n, y_n)$  is not visible in principle,

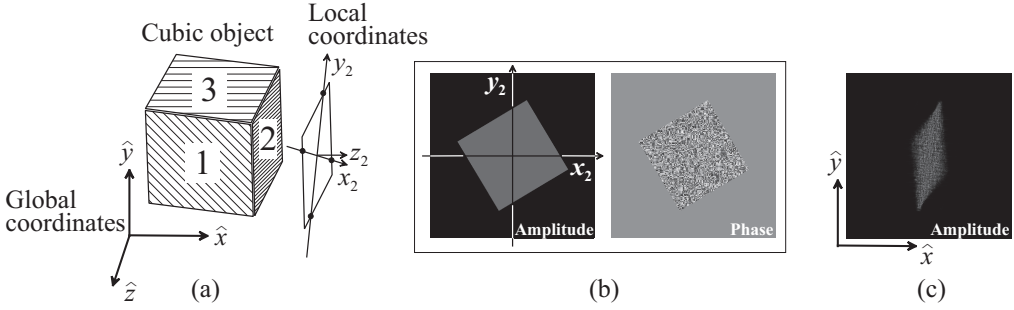


Fig.1 The principle for synthesizing object field by the polygon-based method: (a) The numerical model of a surface object, (b) The surface function for the polygon #2, (c) The polygon field of the polygon #2.

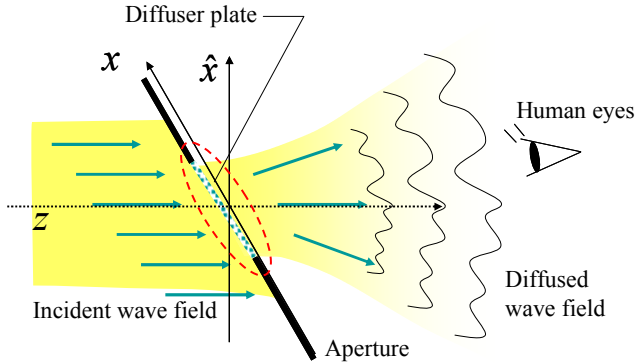


Fig.2 The theoretical model of a polygonal surface source of light.

whereas the amplitude pattern  $a_n(x_n, y_n)$  directly determines the appearance of the polygon. Therefore, the role of the diffuser is performed by the phase pattern. The shape, shade and texture of the polygons come from the amplitude pattern.

### 2.3. Rotational transform and numerical propagation

The surface function of a polygon is yielded from the vertex data of the CG model. Since the surface function is given in a plane not parallel to the hologram, rotational transform [4, 5] that is a numerical technique to propagate fields between non-parallel planes is used for calculating the polygon field in a plane parallel to the hologram. The example of a rotated polygon field is shown in Fig. 1 (c). After rotational transform, the polygon field is shortly propagated by using the band-limited angular spectrum method (BL-AS) to gather all polygon fields in a given plane. This is called an object plane. The BL-AS is a numerical technique proposed for accurate short-distance propagation of wave-fields [6].

The object field that is an entire set of the polygon field in the object plane is then propagated to the hologram plane. However, the hologram plane is usually distant from the object plane and the frame buffer necessary for the object field is commonly too large to simultaneously store in memory. Therefore, the object field is segmented and propagated by using techniques for off-axis numerical

propagation, such as the shifted Fresnel [7] or shifted angular spectrum method [8].

## 3. CAPTURING LARGE-SCALED WAVE-FIELD OF REAL-EXISTENT OBJECTS

The wave-field emitted from a real-existent object is captured by using techniques of digital holography (DH) that is just the digital counterpart of classical holography. The fringe caused by optical interference with a reference wave is digitally recorded by an image sensor instead of light-sensitive materials. Therefore, it is theoretically possible to capture any object field by the DH. However, impressive synthetic holograms commonly need at least more than billions pixels in display resolution and less than one micron in physical resolution [2]. The wave-fields captured by DH do not meet the requirements, because number of the pixels of current image sensor is no more than tens million and the sensor resolution does not reach to less than one micron. To resolve the problem, we use the technique of lensless-Fourier synthetic-aperture digital holography (LFS-A-DH) [3]. This is a type of DH using a spherical reference wave.

### 3.1. The principle for reducing sampling intervals

In the lensless-Fourier DH, the wave-field of an object is obtained by Fourier transform of the captured field, and the sampling intervals  $\Delta_x$  and  $\Delta_y$  of the Fourier-transformed wave-field is given by the following equation in the image plane:

$$\Delta_x = \frac{\lambda d_R}{N_x \delta_x} \text{ and } \Delta_y = \frac{\lambda d_R}{N_y \delta_y}, \quad (1)$$

where  $\lambda$  and  $d_R$  are the wavelength and the distance between the center of the spherical reference wave and the image sensor. Number of the sensor pixels and the sensor pitches are given by  $N_x \times N_y$  and  $\delta_x \times \delta_y$ , respectively. Since the sampling intervals are reduced with increasing the sensor pixels, the technique of the synthetic aperture is used for increasing the effective number of the pixels.

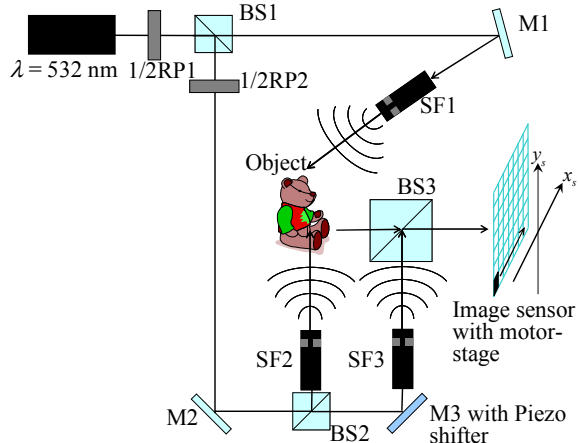


Fig. 3 The experimental setup for capturing large-scaled wave-fields by the LFSA-DH. M: mirror, BS: beam splitter, RP: retarder plate.

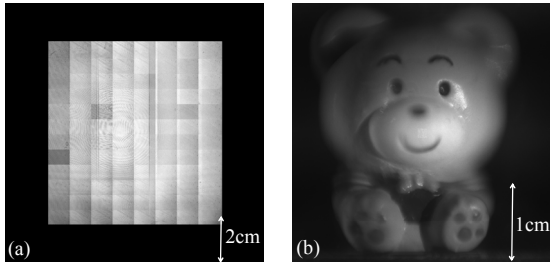


Fig.4 Amplitude images of the captured (a) and Fourier-transformed field (b).

### 3.2. Experiment for capturing large-scaled wave-fields

The experimental setup for capturing large-scaled wave-fields by the LFSA-DH is shown in Fig. 3. The image sensor with  $3000 \times 2200$  pixels (Lumenera Lw625) is mechanically moved by a PC-controlled motor-stage. The fringe pattern is captured 3 times for each position to obtain a complex wave-field using phase-shifts caused by the mirror M3 installed in the Piezo phase-shifter.

Amplitude image of the captured and the Fourier-transformed field are shown in Fig. 4 (a) and (b), respectively. The total field is yielded by stitching individual fields captured at  $8 \times 12$  positions. The total cross section of the captured field is  $7.7 \times 8.0 \text{ cm}^2$ . The parameters used for capturing is summarized in Table 1. Here, the  $d_R$  is the distance between the SF3 generating the reference spherical wave in Fig. 3 and the sensor plane. Since the distance is a free parameter, it is determined by using Eq. (1) so that the sampling intervals of the Fourier-transformed field are  $1.0 \mu\text{m} \times 1.0 \mu\text{m}$ .

In the amplitude image (b) of Fig. 4, the edge of the object is considerably defocused, because the edge is far from the image plane that places around the eyes of the bear object. This blur verifies that the optical wave-field is successfully captured with a wide area.

Table 1 Parameters for capturing the large-scaled field.

Wavelength ( $\lambda$ )	532nm
Sensor pitches ( $\delta_x \times \delta_y$ )	$3.5 \mu\text{m} \times 3.5 \mu\text{m}$
Sampling intervals ( $\Delta_x \times \Delta_y$ )	$1.0 \mu\text{m} \times 1.0 \mu\text{m}$
Total number of samplings ( $N_x \times N_y$ )	$32,768 \times 32,768$
Distance of reference point source ( $d_R$ )	21.5cm

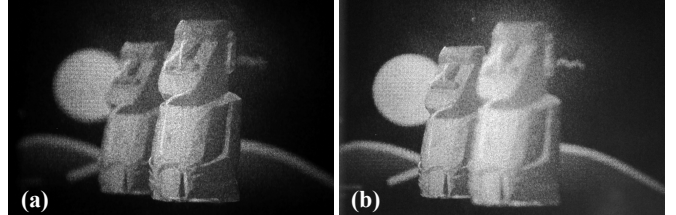


Fig. 5 Optical reconstruction of “Moai II.” The camera is focused on the near moai (a) and the far moai (b).

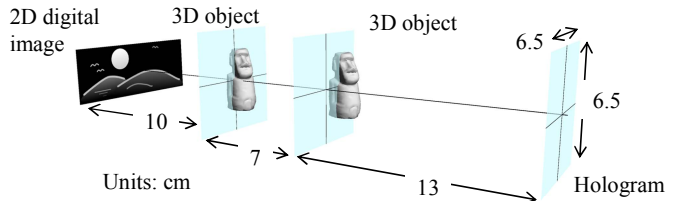


Fig. 6 The 3D scene of “Moai II”

## 4. OPTICAL RECONSTRUCTION OF HOLOGRAMS

Examples of optical reconstruction of a fully synthetic hologram named “Moai II” are shown in Fig. 5. This hologram is created for reconstructing a virtual 3D scene in Fig. 6. The 3D object and the wallpaper are given by a numerical mesh data and a digital image, respectively. Total number of pixels of the Moai II is approximately 4 G pixels ( $\approx 65,536 \times 65,536$ ). Since the pixel pitches are  $1.0 \mu\text{m} \times 1.0 \mu\text{m}$ , the viewing angle is  $37^\circ$  both in horizontal and vertical.

### 4.1. Creation of mixed 3D scene with real objects

The real-existent object, the ornament of a small bear whose wave-field is capture by the LFSA-DH in section 3.2, is mixed with a virtual 3D scene. The design of the scene is shown in Fig. 7. Here, the bear appears twice on the scene, i.e. the same captured wave-field is used twice in the scene. This is impossible in classical holography. Only digitized holography allows us to edit the 3D scene. Some synthetic objects such as wallpaper or 3D bees are arranged behind or in front of the double bear.

The light behind the real-existent object must be shielded to prevent the object from being a see-through phantom image and correctly reconstruct the occluded scene. The silhouette method [2] used for light-shielding in synthetic holography is applied to the real-existent object. The silhouette mask shown in Fig. 8 (b) is produced from the amplitude image in (a). This amplitude image is yielded from a small part of the captured field in order to avoid blur caused in Fig. 4 (b).

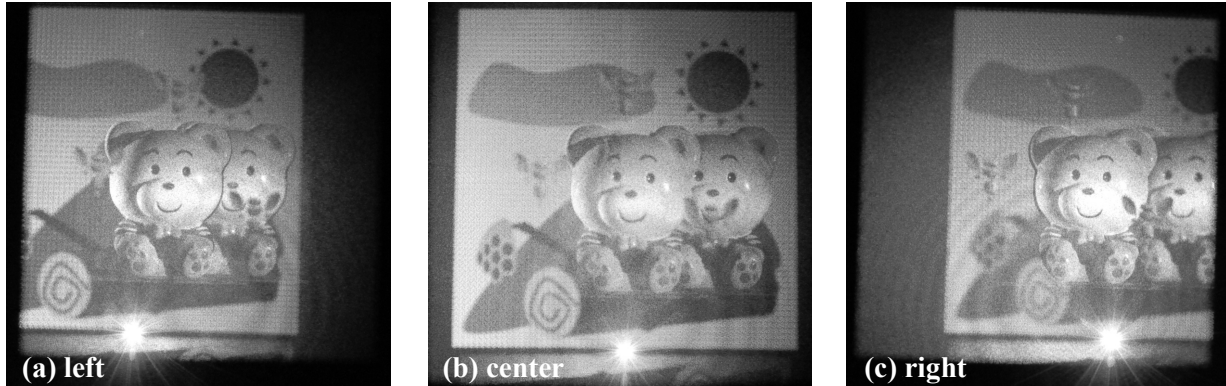


Fig.9 Photographs of optical reconstruction of the “Bear II” hologram created for the mixed 3D scene including real-existent and virtual objects. Photographs (a) – (c) are taken from different view points.

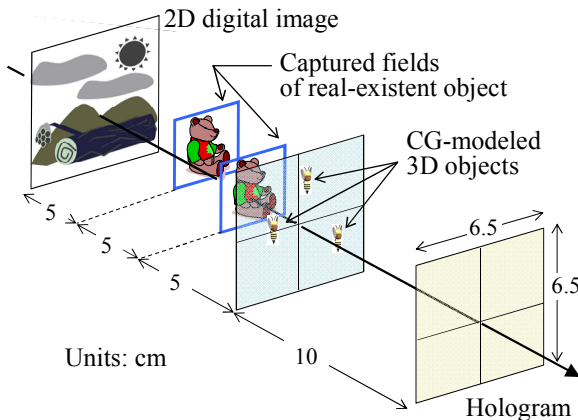


Fig.7 The mixed 3D scene of “Bear II” including the field of the real-existent object and the CG-modeled virtual object.

#### 4.2. Optical reconstruction of mixed 3D scene

The parameters of the hologram, named “Bear II”, are exactly the same as that of the Moai II. After calculation of the total wave-field of the scene, including captured fields, the fringe pattern is generated by numerical interference with the reference wave, and then quantized to produce a binary amplitude hologram. Finally, the hologram is fabricated by using laser lithography system. Photographs of the optical reconstruction of the Bear II are shown in Fig. 9. It is verified that occlusion of the 3D scene is accurately reconstructed in different points of view.

#### 5. CONCLUSION

We proposed a novel technique named digitized holography. The whole process of classical holography is replaced with digital processing in the technique. As a result, the 3D scene reconstructed by holograms can be edited and mixed with CG-modeled virtual object. The reconstructed 3D image is a spatial image and thus gives strong impression to reviewers.

This work was supported by the JSPS.KAKENHI (21500114). The mesh data for the moai objects are

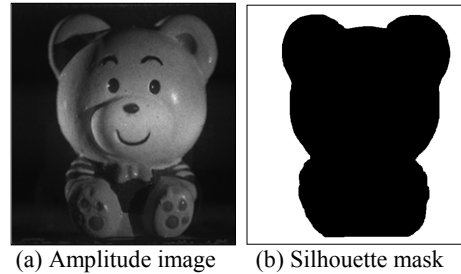


Fig.8 (a) The amplitude image obtained from a small part of the captured field. (b) The silhouette mask produced by the amplitude image.

provided courtesy of Yutaka\_Ohtake by the AIM@SHAPE Shape Repository.

#### 6. REFERENCES

- [1] K. Matsushima, “Computer-generated holograms for three dimensional surface objects with shade and texture,” *Appl. Opt.* **44**, pp. 4607–4614, 2005.
- [2] K. Matsushima and S. Nakahara, “Extremely high-definition full-parallax computer-generated hologram created by the polygon-based method,” *Appl. Opt.* **48**, pp. H54–H63, 2009
- [3] T. Nakatsuji and K. Matsushima, “Free-viewpoint images captured using phase-shifting synthetic aperture digital holography,” *Appl. Opt.* **47**, pp. D136-D143, 2008.
- [4] K. Matsushima, H. Schimmel, and F. Wyrowski, “Fast calculation method for optical diffraction on tilted planes by use of the angular spectrum of plane waves,” *J. Opt. Soc. Am. A* **20**, pp. 1755–1762, 2003.
- [5] K. Matsushima, “Formulation of the rotational transformation of wave fields and their application to digital holography,” *Appl. Opt.* **47**, pp. D110–D116, 2008.
- [6] K. Matsushima and T. Shimobaba, “Band-limited angular spectrum method for numerical simulation of free-space propagation in far and near fields,” *Opt. Express* **17**, pp. 19662–19673, 2009.
- [7] R. P. Muffoletto, J. M. Tyler, and J. E. Tohline, “Shifted Fresnel diffraction for computational holography,” *Opt. Express* **15**, pp. 5631–5640, 2007.
- [8] K. Matsushima, “Shifted angular spectrum method for off-axis numerical propagation,” *Opt. Express* **18**, pp. 18453–18463, 2010.